

Estimation of Left Ventricular Cavity Area With an On-line, Semiautomated Echocardiographic Edge Detection System

Byron F. Vandenberg, MD; Linda S. Rath; Patricia Stuhlmuller, RN; Hewlett E. Melton Jr., PhD; and David J. Skorton, MD

Background. Automated edge detection of endocardial borders in echocardiograms provides objective, reproducible estimation of cavity area; however, most methods have required off-line analysis. A recently developed prototype echocardiographic imaging system permits real-time automated edge detection during imaging and thus, the potential for measurement of cyclic changes in cavity area and the assessment of left ventricular function on-line. Our purpose was to compare measurements of endocardial area manually traced from conventional echocardiograms with those obtained with the real-time automated edge detection system in normal subjects.

Methods and Results. Two training sets of images were used to establish optimal methods of gain setting; the settings were then evaluated in a test set of images. In the high-gain training group ($n=8$ subjects, 119 images), gain settings were adjusted sufficiently high to display at least 90% of the endocardial border. Manually drawn and real-time area measurements correlated at $r=0.92$, but manually drawn areas were underestimated by computer. In the low-gain training group ($n=7$ subjects, 104 images), gain settings were adjusted sufficiently low to avoid cavity clutter despite the presence of dropout of endocardial edges. Manually drawn and real-time areas again correlated ($r=0.79$), but manually drawn areas were overestimated by computer. In the intermediate-gain test group ($n=7$ subjects, 105 images), gain settings were balanced between maximal endocardial definition ($\geq 90\%$) and minimal cavity clutter ($\leq 1 \text{ cm}^2$). Manually drawn and real-time areas correlated at $r=0.91$ for the group, and r ranged from 0.94 to 0.99 in individual subjects. Interobserver variability was 9.5% for manually traced areas and 10.6% for real-time area measurements.

Conclusions. Real-time, on-line automated edge detection provides accurate estimation of manually drawn cavity areas. Although the method is gain dependent, measurements are reproducible. The system should have clinical application in settings in which measurements of left ventricular function are important. (*Circulation* 1992;86:159-166)

KEY WORDS • echocardiography • left ventricle • edge detection • computers

The use of imaging techniques for quantification of cardiac structure or dynamics requires identification of borders. The detection of endocardial borders permits the measurement of cardiac areas, volumes or ejection fractions,^{1,2} and the recognition of abnormal endocardial motion in the presence of ischemia or infarction.³⁻⁶ Manual border tracing, however, is tedious and subjective, with a variability of 5-10% in area measurement.⁷⁻⁹ Thus, most clinical echocardiographers do not routinely perform quantification based on endocardial border definition. Investigators have proposed ways to

automate the process of border identification^{7,10-22} to reduce errors and analysis time, but most of the methods have required off-line computer analysis, and as a consequence, these automated border detection techniques have received limited clinical application.

A recently developed prototype echocardiographic imaging system permits real-time automated edge detection with on-line cavity area measurement throughout the cardiac cycle. Our purpose was to test the hypothesis that measurements of endocardial area obtained with the prototype system would correlate with those manually traced from conventional two-dimensional echocardiograms.

Methods

Echocardiography

A Hewlett-Packard Sonos 1000 ultrasound machine was modified with hardware and software for real-time edge detection (Figure 1) based in part on earlier work from our laboratory.¹⁶ Imaging was performed with a 2.5- or 3.5-MHz, 64-element phased-array transducer. The received radiofrequency signal was converted to a power signal, and this was compared with a threshold

From The Cardiovascular Center, Departments of Internal Medicine and Electrical and Computer Engineering (B.F.V., L.S.R., P.S., D.J.S.), The University of Iowa, Iowa City; and Hewlett-Packard Laboratories (H.E.M.), Palo Alto, Calif.

Supported in part by Specialized Center of Research in Coronary and Vascular Diseases grant P50-HL-32295; Research Career Development award K04-HL-01290 (D.J.S.); and American Heart Association grant-in-aid (Iowa Affiliate, West Des Moines) IA-88-G-39 (B.F.V.).

Address for reprints: Byron F. Vandenberg, MD, Department of Internal Medicine, University of Iowa Hospital, Iowa City, IA 52242.

Received November 11, 1991; revision accepted March 17, 1992.

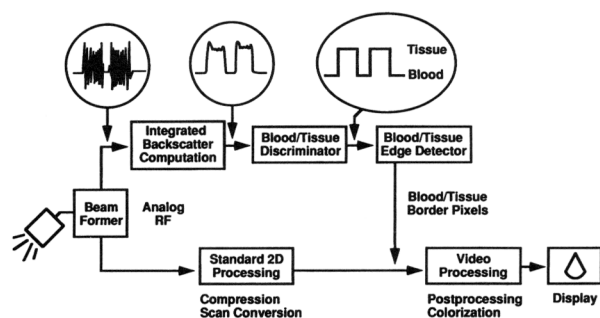


FIGURE 1. Block diagram of the automated border detection system. The received radiofrequency (RF) signals from each scan line are converted to integrated backscatter (i.e., power signal). The power signals from tissue and blood are discriminated by comparing the signals with a threshold level. Border pixels are then assigned to the tissue–blood interfaces. Automated borders are superimposed on the conventional two-dimensional (2D) echocardiographic images and displayed in real time on the video monitor.

for locating the tissue–blood interfaces along each scan line (Figure 1). Edge signals were displayed on conventional or backscatter video images in real time. Data were obtained using a system modification used in previous studies.^{23–30}

The operator adjusted the transmit power and time-gain compensation controls in order to approximate the automated borders to the visually apparent endocardial surface; operator interaction is necessary to ensure that borders are appropriately placed at tissue–blood interfaces rather than at edges of acoustic artifacts. Once adjustments are judged satisfactory (see below), a track-ball-derived region of interest (ROI) was placed to include the short-axis endocardial circumference at end diastole. The area was then measured in real time from the endocardial contour and displayed as a waveform representing the cavity area within the ROI throughout the cardiac cycle.

Protocol

Conventional two-dimensional echocardiograms were performed during held expiration. Normal subjects with parasternal short-axis views of the left ventricle in which at least 75% of the endocardium was clearly seen were selected for study.^{31,32} Imaging was repeated with the real-time border detection system. Transmit power and time-gain compensation were adjusted according to criteria discussed below, in which two training sets of images were used to establish optimal methods of gain setting and were then evaluated in a test set of images.

Subjects

All subjects (mean age, 31 ± 3 years) had normal history and physical examinations. No subjects were taking cardiac medications. One subject was studied at all gain settings; otherwise each subject had only one study.

High-gain training group. In the initial group of eight normal subjects studied with the real-time system, time-gain compensation and transmit power were adjusted sufficiently high to display at least 90% of the endocardial border circumference identified by conventional echocardiography (Figure 2). The demonstration of real-time endocardial borders was attempted despite the presence of signal from within the ventricular cavity (i.e., clutter).

Low-gain training group. In the second group of seven normal subjects, time-gain compensation and transmit power were adjusted sufficiently low to avoid cavity clutter despite the presence of dropout of endocardial edges (Figure 3). To approximate the regions of endocardial dropout, the ROI was drawn along the assumed endocardial circumference, approximately in end diastole.

Intermediate-gain test set. Based on data from the training sets (see “Results”), it became apparent that a balance between maximal endocardial definition and minimal cavity clutter was necessary. In the test set of seven normal subjects, transmit power and time-gain compensation were adjusted to again limit cavity clutter

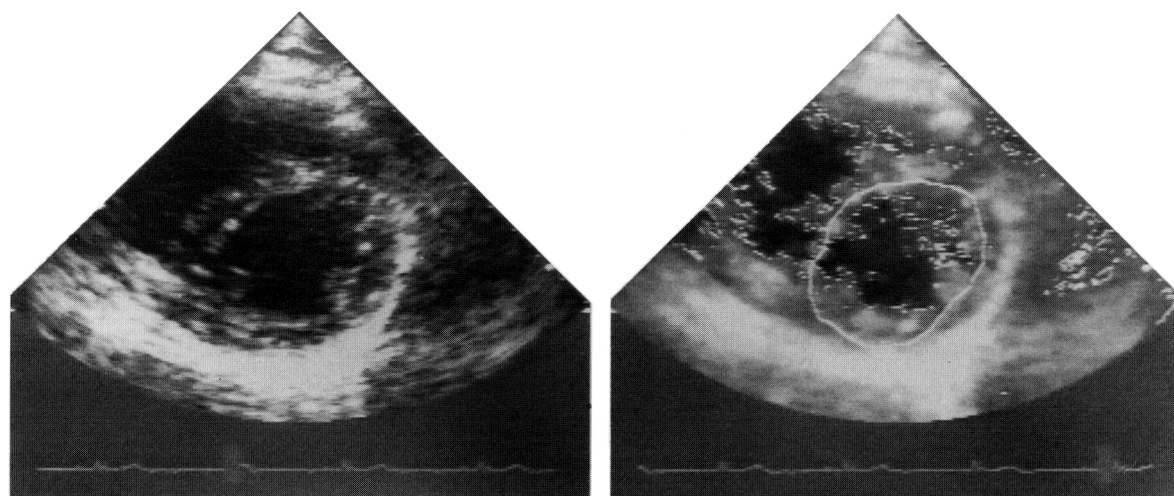


FIGURE 2. Images from the high-gain training group. Left panel: Conventional echo of left ventricle (parasternal short-axis view). The endocardial edge was considered to be the interface between the bright endocardial echoes and the dark cavity of the left ventricle. Right panel: Real-time border detection system. To identify endocardial interfaces parallel to the ultrasound beam (i.e., medial and lateral walls), increased transmit and time-gain compensation was necessary, leading to the appearance of cavity clutter.

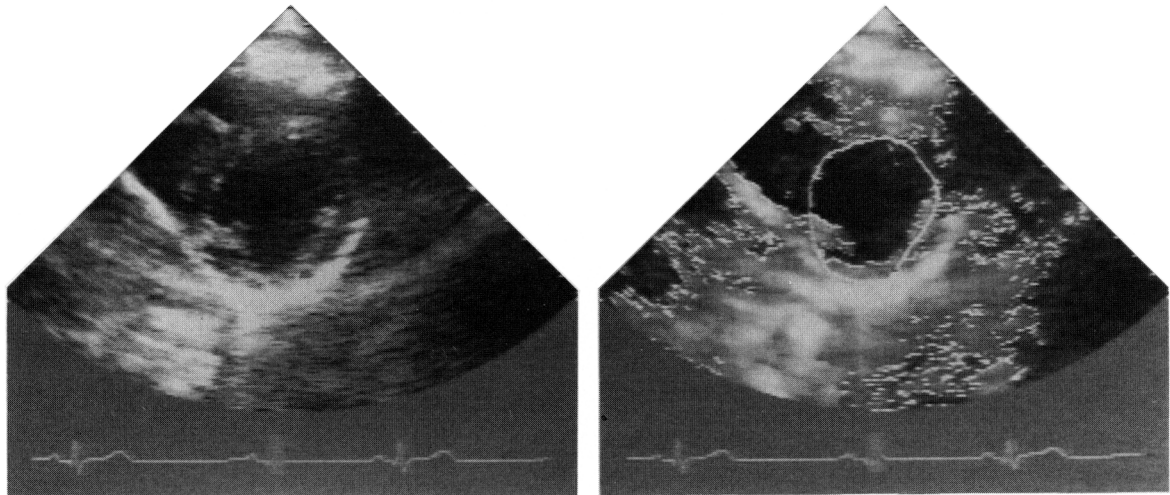


FIGURE 3. Images from the low-gain training group. Left panel: Conventional echo of left ventricle (parasternal short-axis view). Right panel: Real-time border detection system. Because of the relatively weaker signal returning from the medial and lateral walls, dropout in the endocardial real-time border occurred.

to approximately $\leq 1 \text{ cm}^2$ and to display at least 90% of the endocardial circumference (Figure 4).

To assess interobserver variability, a second investigator repeated imaging with the real-time border detection system in four of the subjects. The investigator viewed the short-axis level imaged by the initial investigator after transmit power and time-gain compensation were reset to zero. Thus, the second investigator repeated the entire process of image acquisition and instrument adjustments.

Measurements

Endocardial borders of the conventional echocardiograms were manually traced by an observer blinded to the instrument-generated borders. Manual tracing was done using the trailing edge-to-leading edge method,^{11,12,14} drawing the borders at the tissue (endocardial)-blood (cavity) interface; the cavity area border was traced along the interface between the white (endocardial) and black (cavity) pixels. The papillary mus-

cles were not included in the cavity area. Areas were traced from serial frames (30 frames per second) from the electrocardiographic QRS onset until the end of systole (defined as the smallest apparent cavity area). Areas were traced from a single cycle. A second observer traced the images obtained in four subjects by the initial observer to determine interobserver variability of manual tracing.

Real-time areas were determined by measurements made from the waveforms generated by the real-time border detection system and recorded on videotape (Figure 5). Measurements were obtained from a single waveform, using the system's measurement features; a trackball was used to measure the distance from baseline to the area waveform on serial frames after the QRS complex.

Data Analysis

Manually drawn versus real-time areas were compared with linear regression analysis, matching area

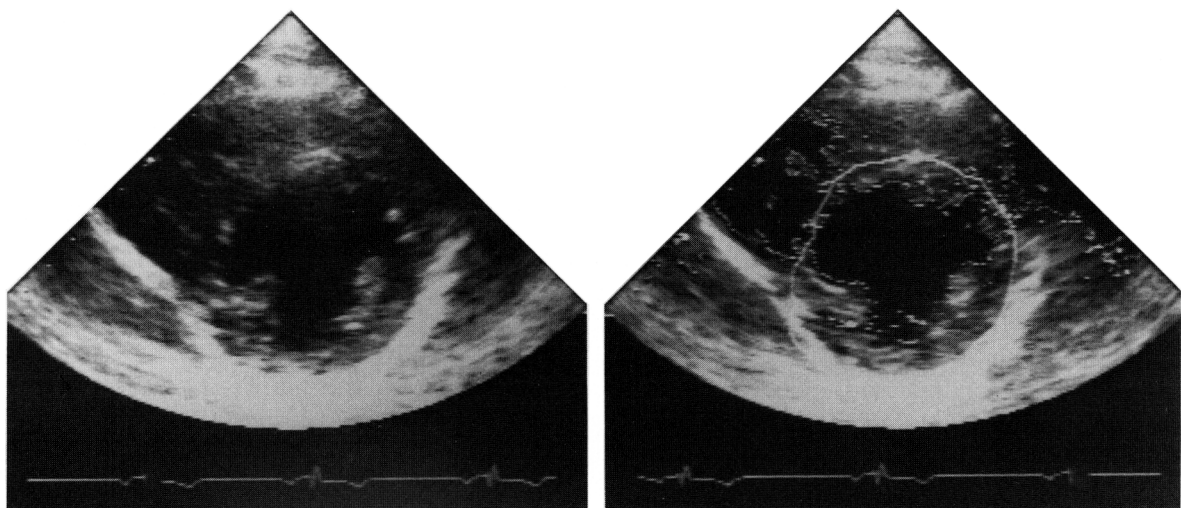


FIGURE 4. Images from the intermediate-gain test group. Left panel: Conventional echo of left ventricle (parasternal short-axis view). Right panel: Real-time border detection system.

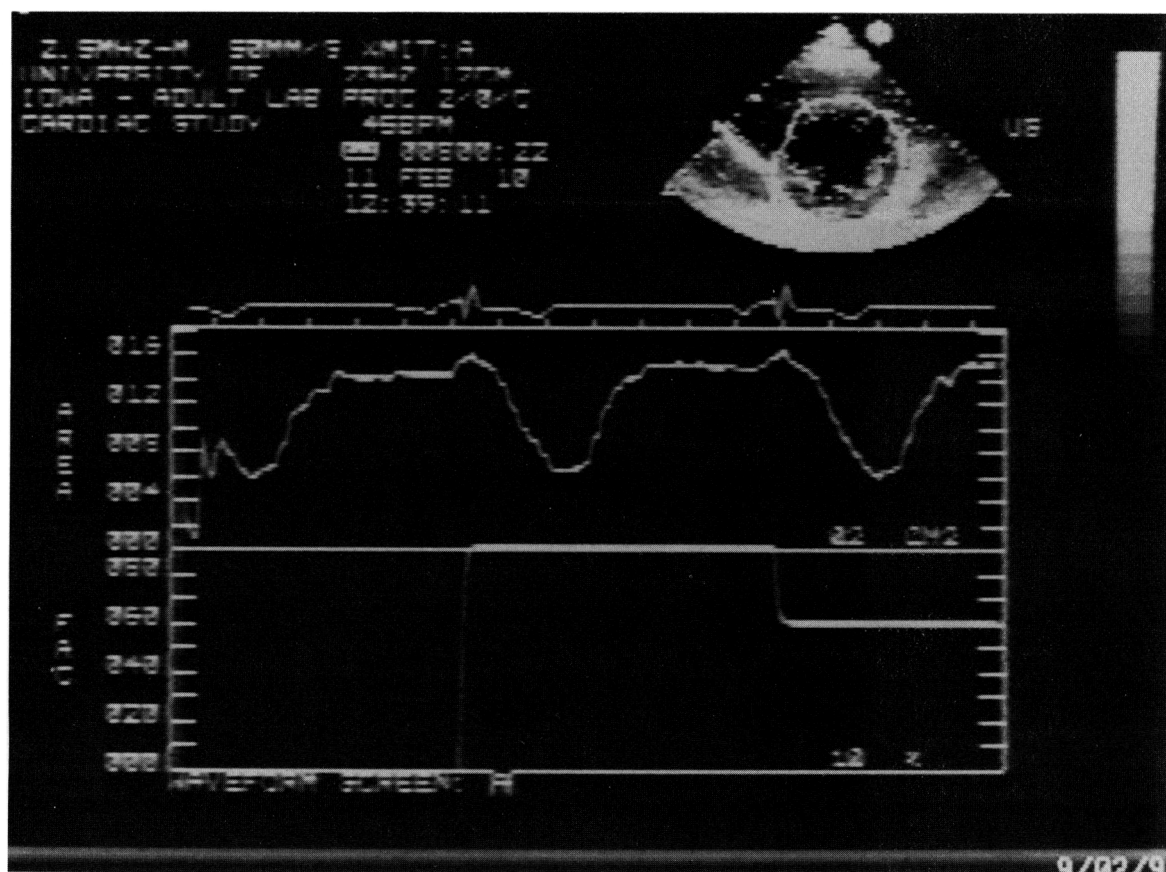


FIGURE 5. Waveform display of areas measured in a normal subject, using intermediate-gain settings.

measurements using the QRS onset as a common reference point to obtain measurements at corresponding points in the cardiac cycle. Interobserver variability was expressed as the difference of two measurements divided by the mean value $\times 100$. Student's *t* test was used to compare significance ($p < 0.01$) of differences between groups.

Results

Thirty-seven individuals were imaged, but only 22 (60%) had $\geq 75\%$ of the endocardium visualized. Twelve to 17 frames during systole were compared in each subject. The time required to manually trace areas was 7.5 ± 2.1 minutes compared with 2.1 ± 0.6 minutes for measuring areas from the real-time area waveforms ($p < 0.05$).

High-Gain Training Group

Manually drawn and real-time area measurements correlated at $r = 0.92$ in the eight subjects (Figure 6). However, because of the y-intercept of -1.28 cm^2 and the underestimation of the manually drawn areas, videotape recordings were reviewed. One half of the eight normal subjects studied had $> 1 \text{ cm}^2$ of cavity clutter. One square centimeter was chosen to separate the groups because it provided a visually apparent stratification of subjects into those with acceptable versus excessive cavity clutter. After excluding the four subjects with $> 1 \text{ cm}^2$ of clutter, manually drawn and real-time areas correlated at $r = 0.97$ with a y intercept of 0.59 cm^2 (Figure 7).

Low-Gain Training Group

In the normal subjects studied at low gain, the manually drawn and real-time areas correlated at $r = 0.79$, with a large y-intercept of 7.46 cm^2 (Figure 8) caused by endocardial dropout.

Intermediate-Gain Test Group

In the test group, manually drawn and real-time areas correlated at $r = 0.91$ (Figure 9). In individual subjects, manually drawn and real-time areas correlated with $r = 0.94$ – 0.99 (Figure 10 and Table 1).

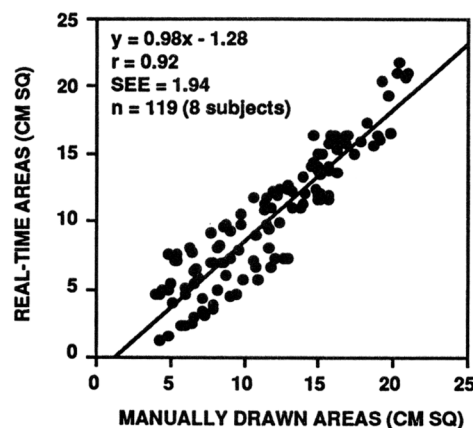


FIGURE 6. Scatterplot shows comparison of real-time and manually drawn areas in the high-gain training group.

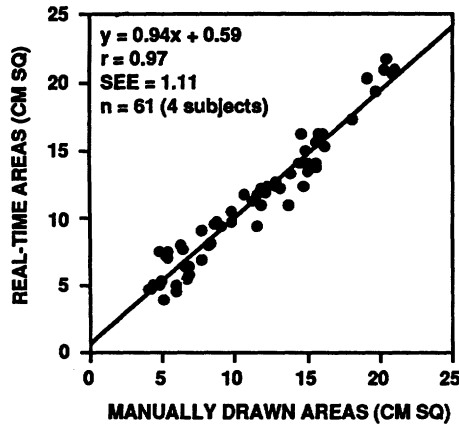


FIGURE 7. Scatterplot shows comparison of real-time and manually drawn areas in the high-gain training group, excluding subjects with $>1 \text{ cm}^2$ of cavity clutter.

Variability

Four subjects in the intermediate-gain test group had studies performed by two different operators. The interobserver variability of manually traced areas was $9.5 \pm 7.5\%$. The interobserver variability of real-time area measurements was $10.6 \pm 8.7\%$ ($p = \text{NS}$).

Discussion

Previous approaches to automated edge detection in echocardiography have been developed to improve the accuracy and reproducibility of border detection in echocardiography.⁸ The computerized methods used in the automated analysis of echocardiographic images fall under the general category of image processing procedures known as segmentation.³³ These methods are intended to separate a particular object or ROI (e.g., the left ventricular [LV] cavity) from another object (e.g., the myocardium). A simple approach to image segmentation is to separate the image into two regions based on the gray level values of their picture elements (pixels) compared with some particular threshold value.^{10,11} Thus, pixels with gray levels above the threshold will be considered part of one region (e.g., myocardium), whereas pixels below the threshold will be considered part of the other region (e.g., LV cavity).

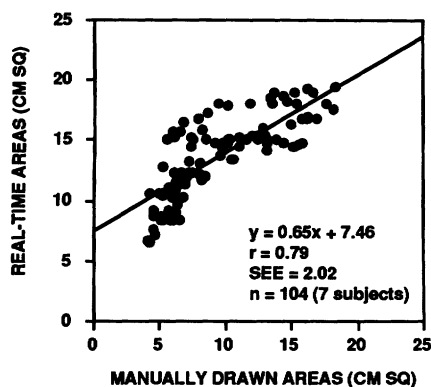


FIGURE 8. Scatterplot shows comparison of real-time and manually drawn areas in the low-gain training group.

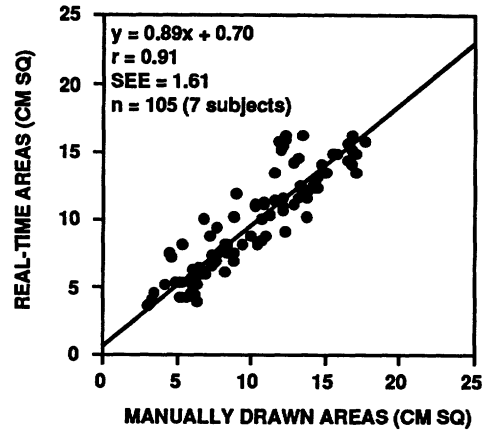


FIGURE 9. Scatterplot shows comparison of real-time and manually drawn areas in the intermediate-gain test group.

More recent approaches to segmentation in echocardiography have not identified regions but instead delineate boundaries between regions; these techniques are referred to as border or edge detection techniques.⁸

Traditional border detection methods consist of two general operations. First, all pixels in the image are evaluated for their potential to represent points on the boundary.³³ The boundary between the two regions of a binary image resulting from gray level thresholding may be considered a high-probability region for a border. Alternatively, a gradient or change in gray level across pixels may define a high likelihood that a pixel represents an edge.^{11,12,14} More complex methods have used the rate of change (first derivative) of gray level values as well as combinations of gray level gradients with gray level thresholding. Regardless of the particular method of assessing the likelihood that each pixel represents an important edge in the image, the result of this first operation is a numerical representation of the image in which each pixel's gray level value is replaced by the likelihood that that pixel represents an edge in the image.

The second step in traditional border detection methods is to decide which pixels have edge likelihoods sufficiently high to be defined as image borders.³³ For example, if each pixel represents a change in gray level across a portion of an image, some threshold value for gray level gradient may be required to consider a pixel as actually representing a border.

After the likelihood of edge identification is established, edge points must sometimes be connected or interpolated in areas of gaps or image dropouts. The connected edge points produce a continuous set of borders.⁸

Several variations on the above-mentioned approaches have been used with varying degrees of success in echocardiographic border detection. Skorton et al¹⁰ reported an early global gray level thresholding approach to echocardiographic edge detection. This technique showed some success, but regional image brightness variations related to noise or image dropout limited the reliability of the method. Garcia et al¹² developed a method of real-time computerization of two-dimensional echocardiography including image smoothing and gray level thresholding combined with second derivative edge detection methods. This method resulted in a near real-time analysis of LV cavity geometry. Collins et al¹¹ compared the accuracy of

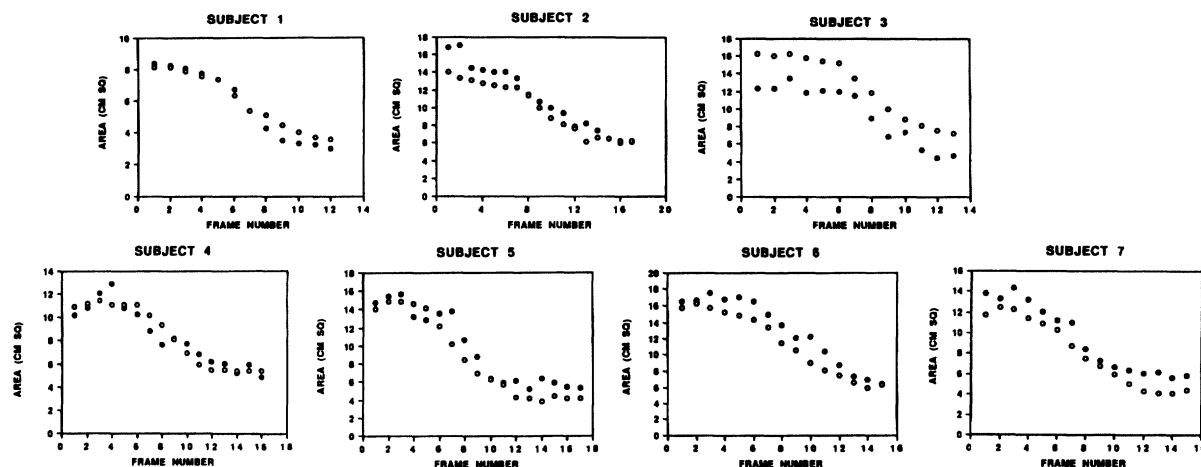


FIGURE 10. Plots show comparisons of real-time (open circles) and manually drawn (solid circles) waveforms in normal subjects.

four different computerized methods of border detection with anatomic data; each of the methods accurately identified endocardial and epicardial borders in vitro. Zhang and Geiser^{21,22} developed a promising algorithm that included search region limitation based on user interaction followed by border detection. In part, this method was based on the amount of motion found in endocardial or epicardial border points from frame to frame. Chu et al¹⁸ reported methods of edge detection based on gradient measurements and also emphasized the importance of redundant information from previous frames to aid in the definition of edges in the current frame.

Although extremely promising, virtually all of these methods necessitate off-line analysis, requiring at least several minutes to derive reliable border data. The main contribution of the presently reported technique is the extraction of meaningful geometric data during the echocardiographic examination so that the information on LV size and function is available immediately to the echocardiographer.

Real-time, On-line Border Detection

With the current method, tissue-blood segmentation is determined from a threshold comparison applied directly to the ultrasound signal power¹⁶ rather than to gray level values of a digitized video image. The signal power is derived from the radiofrequency signal. This approach is similar to the previous work because both make use of a threshold in deciding between tissue and cavity; however, the current approach uses an estimate of signal power, unlike the previous approach.¹⁶

In the current method, the best endocardial contour is identified by the operator, matching the instrument border contour to the endocardium of the two-dimensional image by using gain and transmit power adjustment. The operator also identifies the cavity of interest by drawing an ROI around the cavity so that the cavity is contained within the ROI throughout the cardiac cycle.

Comparisons With Manual Methods of Cavity Area Measurement

We studied the performance of the edge operator in only the short-axis views of the LV for several reasons: 1) With short-axis view imaging, myocardial regions perfused by the three coronary arteries are separable, and therefore the view is important during LV function monitoring. 2) Real-time, on-line edge detection is difficult to perform in the apical and long-axis views because of valve motion. For example, while monitoring LV cavity area with an apical four-chamber view, mitral valve leaflets move into the chamber during diastole. Because borders are assigned to the valve leaflet-blood interface, the area occupied by the valves is not included in the detected cavity area. Because the contribution to the cavity area varies according to whether the valve is open or closed, the error is not consistent and therefore cannot be corrected.

In our study, cavity areas derived from the real-time method were compared with areas obtained with the trailing edge-to-leading edge tracing methodology. That is, the cavity area was traced between the white pixels of the endocardium and the black pixels of the ventricular cavity. Thus, the visually apparent endocardial tissue-blood interface was traced. The leading edge-to-leading edge method may represent a more accurate estimate of the true cavity area because of ultrasound beam width spreading and encroachment of edges into the ventricular cavity.^{12,34-38} We chose the trailing edge-to-leading edge method because 1) the trailing edge-to-leading edge method and some edge detection algorithms both identify similar boundaries (i.e., the tissue-blood interface); 2) while the trailing edge-to-leading edge method yields a consistent underestimation of the true areas, the correlations are similar to the leading edge-to-leading edge methods³⁵; and 3)

TABLE 1. Waveform Correlations (Manual vs. Real-time) in Individual Subjects

Subject	<i>r</i>	SEE (cm ²)	Regression equation
1	0.99	0.25	$y = 0.81x + 1.29$
2	0.97	0.69	$y = 0.77x + 1.34$
3	0.98	0.68	$y = 1.08x + 2.28$
4	0.94	0.94	$y = 0.97x + 0.23$
5	0.96	1.29	$y = 1.05x - 1.57$
6	0.98	0.79	$y = 0.93x - 0.65$
7	0.99	0.55	$y = 0.97x - 1.11$

definition of the leading edge-to-leading edge boundary may be associated with excessive variability.³⁴

Papillary muscles were not included in the manually traced measurements of the short-axis cavity area; that is, instead of tracing the endocardium in the regions of the papillary muscles, borders were traced along the papillary muscle-blood interface. Most investigators have had similar approaches to border detection.¹⁴ Geiser et al,^{7,13} however, applied an edge detection algorithm that relied on operator-defined regions of search; thus, papillary muscles could be included in the cavity area measurements. The interobserver variability with this method was attributed to variations in tracing the perceived endocardial border in the region of the papillary muscles.

The real-time border detection system accurately estimated manually drawn cavity areas in the test group of normal subjects, and the correlation was excellent in each of the individuals, with r ranging from 0.94 to 0.99. The accuracy of estimating cavity areas in individual subjects is particularly relevant to clinical applications in which decisions regarding patient management depend on consistently precise measurement.

Similar correlations in the comparison between manually drawn and edge detection methods were obtained by Zwehl et al.¹⁴ In their study of edge detection methods applied to digitized short-axis LV images of dogs, the slope of the correlations approached unity, with $r=0.91$ and 0.92 and $SEE=1.6$ and 1.34 cm^2 at end diastole and end systole, respectively. In their method, however, areas of echo dropout were filled in manually. In the method described in our study, areas of dropout were measured as cavity area. That is, in the absence of a tissue-blood interface, the cavity area extended to the ROI. This may explain the overestimation of area in some patients (e.g., subject 3). In addition, the absence of "gap filling" readily explains the overestimation of the manually drawn areas in the low-gain test group. The underestimation of cavity areas in the initial high-gain training group was presumably related to the identification of tissue-blood interfaces in areas of excessive cavity clutter. Linker et al³⁹ demonstrated variation in the appearance of the gray level histogram at low-, intermediate-, and high-gain settings³⁹ and recommended an intermediate gain for optimizing threshold procedures.

The interobserver variability in manual tracing of the endocardial borders was 9.5%, in the range of previously reported values.⁷⁻⁹ This variability was similar to the variability in area measurements obtained by different observers with the real-time system.

Limitations

Cavity clutter and endocardial dropout are the major problems in this method of automated border detection. Future improvements should include 1) deletion or thinning of isolated or extraneous edge pixels,¹¹ 2) rational gain compensation in order to optimally vary gain settings according to regional variations in the attenuation of ultrasound,^{16,40} and 3) on-line differentiation of area waveforms to provide indexes of LV function.¹²

The current study was performed in the parasternal short-axis view because this view seemed least likely to introduce errors from valve motion. Because coronary

artery disease may produce infarction and wall motion abnormality in regions that are not imaged from the short-axis view, further work is necessary in other imaging planes before assuming that automated border detection is valid in all imaging planes.

Conclusions

Real-time, on-line automated edge detection provides accurate estimation of manually drawn cavity areas. Although the method is gain dependent, requiring operator interaction and judgment, real-time area measurements are reproducible; the correlations with manually drawn cavity areas are consistently excellent for individuals ($r=0.94-0.99$). The system should have clinical application in settings in which measurements of LV function are important, particularly for assessing real-time variations in ventricular function and averaging measurements from multiple cycles.

Acknowledgment

We acknowledge the expert secretarial assistance of Diane Phillips in the preparation of the manuscript.

References

- Wyatt HL, Heng MK, Meerbaum S, Gueret P, Hestenes J, Dula E, Corday E: Cross-sectional echocardiography: II. Analysis of mathematic models for quantifying volume of the formalin-fixed left ventricle. *Circulation* 1980;61:1119-1125
- Folland ED, Parisi AF, Moynihan PF, Jones DR, Feldman CL, Tow DE: Assessment of left ventricular ejection fraction and volumes by real-time, two-dimensional echocardiography: A comparison of cineangiographic and radionuclide techniques. *Circulation* 1979;60:760-766
- Pandian NG, Kieso RA, Kerber RE: Two-dimensional echocardiography in experimental coronary stenosis: II. Relationship between systolic wall thinning and regional myocardial perfusion in severe coronary stenosis. *Circulation* 1982;66:603-611
- Heger JJ, Weyman AE, Wann LS, Dillon JC, Feigenbaum H: Cross-sectional echocardiography in acute myocardial infarction: Detection and localization of regional left ventricular asynergy. *Circulation* 1979;60:531-538
- Parisi AF, Moynihan PF, Folland ED, Feldman CL: Quantitative detection of regional left ventricular contraction abnormalities by two-dimensional echocardiography: II. Accuracy in coronary artery disease. *Circulation* 1981;63:761-767
- Weiss JL, Bulkley BH, Hutchins GM, Mason SJ: Two-dimensional echocardiographic recognition of myocardial injury in man: Comparison with postmortem studies. *Circulation* 1981;63:401-408
- Geiser EA, Oliver LH, Gardin JM, Kerber RE, Parisi AF, Reichel N, Werner JA, Weyman AE: Clinical validation of an edge detection algorithm for two-dimensional echocardiographic short-axis images. *J Am Soc Echocardiogr* 1988;1:410-421
- Skorton DJ, Collins SM, Garcia E, Geiser EA, Hillard W, Koopes W, Linker D, Schwartz G: Digital signal and image processing in echocardiography. *Am Heart J* 1985;110:1266-1283
- Moynihan PF, Parisi AF, Feldman CL: Quantitative detection of regional left ventricular contraction abnormalities by two-dimensional echocardiography: I. Analysis of methods. *Circulation* 1981;63:752-760
- Skorton DJ, McNary CA, Child JS, Newton FC, Shah PM: Digital image processing of two dimensional echocardiograms: Identification of the endocardium. *Am J Cardiol* 1981;48:479-486
- Collins SM, Skorton DJ, Geiser EA, Nichols JA, Conetta DA, Pandian NG, Kerber RE: Computer-assisted edge detection in two-dimensional echocardiography: Comparison with anatomic data. *Am J Cardiol* 1984;53:1380-1387
- Garcia E, Gueret P, Bennett M, Corday E, Zwehl W, Meerbaum S, Corday S, Swan HJC, Berman D: Real-time computerization of two-dimensional echocardiography. *Am Heart J* 1981;101:783-792
- Geiser EA, Conetta DA, Limacher MC, Stockton VO, Oliver LH, Jones B: A second generation computer-based edge detection algorithm for short-axis two-dimensional echocardiographic images: Accuracy and improvement in interobserver variability. *J Am Soc Echocardiogr* 1990;3:79-90

14. Zwehl W, Levy R, Garcia E, Haendchen RV, Childs W, Corday SR, Meerbaum S, Corday E: Validation of a computerized edge detection algorithm for quantitative two-dimensional echocardiography. *Circulation* 1983;68:1227-1235
15. Buda AJ, Delp EJ, Meyer CR, Jenkins JM, Smith DN, Bookstein FL, Pitt B: Automatic computer processing of digital two-dimensional echocardiograms. *Am J Cardiol* 1983;52:384-389
16. Melton HE Jr, Collins SM, Skorton DJ: Automatic real-time endocardial edge detection in two-dimensional echocardiography. *Ultrason Imaging* 1983;5:300-307
17. Delp EJ, Buda AJ, Swastek MR, Smith DN, Jenkins JM, Meyer CR, Pitt B: The analysis of two-dimensional echocardiograms using a time-varying image approach. *Comput Cardiol, IEEE* 1982: 391-394
18. Chu CH, Delp EJ, Buda AJ: Detecting left ventricular endocardial and epicardial boundaries by digital two-dimensional echocardiography. *IEEE Trans Med Imaging* 1988;7:81-90
19. Jenkins JM, Qian G, Besozzi M, Delp EJ, Buda AJ: Computer processing of echocardiographic images for automated edge detection of left ventricular boundaries. *Comput Cardiol, IEEE* 1981: 391-394
20. Conetta DA, Geiser EA, Oliver LH, Miller AB, Conti RC: Reproducibility of left ventricular area and volume measurements using a computer endocardial edge-detection algorithm in normal subjects. *Am J Cardiol* 1985;56:947-952
21. Zhang LF, Geiser EA: An effective algorithm for extracting serial endocardial borders from two-dimensional echocardiograms. *IEEE Trans Biomed Eng* 1984;31:441-447
22. Zhang LF, Geiser EA: An approach to optimal threshold selection on a sequence of two-dimensional echocardiographic images. *IEEE Trans Biomed Eng* 1982;4:577-581
23. Vandenberg BF, Stuhlmuller JE, Rath L, Kerber RE, Collins SM, Melton HE, Skorton DJ: Diagnosis of recent myocardial infarction with quantitative backscatter imaging: Preliminary studies. *J Am Soc Echocardiogr* 1991;4:10-18
24. Vandenberg BF, Kieso RA, Fox-Eastham K, Kerber RE, Melton HE Jr, Collins SM, Skorton DJ: Characterization of acute experimental left ventricular thrombi with quantitative backscatter imaging. *Circulation* 1990;81:1017-1023
25. Vandenberg BF, Rath L, Shoup TA, Kerber RE, Collins SM, Skorton DJ: Cyclic variation of ultrasound backscatter in normal myocardium is view-dependent: Clinical studies with a real-time backscatter imaging system. *J Am Soc Echocardiogr* 1989;2: 308-314
26. Vered Z, Mohr GA, Barzilai B, Gessler CJ, Wickline SA, Wear KA, Shoup TA, Weiss AN, Sobel BE, Miller JG, Perez JE: Ultrasound integrated backscatter tissue characterization of remote myocardial infarction in human subjects. *J Am Coll Cardiol* 1989; 13:84-91
27. Milunski MR, Mohr GA, Perez JE, Vered Z, Wear K, Gessler CJ, Sobel BE, Miller JG, Wickline SA: Ultrasonic tissue characterization with integrated backscatter: Acute myocardial ischemia, reperfusion, and stunned myocardium in patients. *Circulation* 1989; 80:491-503
28. Vered Z, Barzilai B, Mohr GA, Thomas LJ, Genton R, Sobel BE, Shoup TA, Melton HE Jr, Miller JG, Perez JE: Quantitative ultrasonic tissue characterization with real-time integrated backscatter imaging in normal human subjects and in patients with dilated cardiomyopathy. *Circulation* 1987;76:1067-1073
29. Masuyama T, St Goar FG, Tye TL, Oppenheim G, Schnittger I, Popp RL: Ultrasonic tissue characterization of human hypertrophied hearts in vivo with cardiac cycle-dependent variation in integrated backscatter. *Circulation* 1989;80:925-934
30. Masuyama T, Valantine HA, Gibbons R, Schnittger I, Popp RL: Serial measurement of integrated ultrasonic backscatter in human cardiac allografts for the recognition of acute rejection. *Circulation* 1990;81:829-839
31. Schnittger I, Fitzgerald PJ, Daughters GT, Ingels NB, Kantrowitz NE, Schwarzkopf A, Mead CW, Popp RL: Limitations of comparing left ventricular volumes by two-dimensional echocardiography, myocardial markers and cineangiography. *Am J Cardiol* 1982;50: 512-519
32. Gordon EP, Schnittger I, Fitzgerald PJ, Williams P, Popp RL: Reproducibility of left ventricular volumes by two-dimensional echocardiography. *J Am Coll Cardiol* 1983;2:506-513
33. Fleagle SR, Skorton DJ: Quantitative methods in cardiac imaging: An introduction to digital image processing, in Marcus ML, Schelbert HR, Skorton DJ, Wolf GL (eds): *Cardiac Imaging*. Philadelphia, WB Saunders Co, 1991, pp 72-86
34. Conetta DA, Geiser EA, Skorton DJ, Pandian NG, Kerber RE, Conti CR: In vitro analysis of boundary identification techniques used in quantification of two-dimensional echocardiograms. *Am J Cardiol* 1984;53:1374-1379
35. Wyatt HL, Haendchen RV, Meerbaum S, Corday E: Assessment of quantitative methods for two-dimensional echocardiography. *Am J Cardiol* 1983;52:396-401
36. Roelandt J, van Dorp WG, Bom N, Laird JD, Hugenholtz PG: Resolution problems in echocardiography: A source of interpretation errors. *Am J Cardiol* 1976;37:256-262
37. Helak JW, Reichek N: Quantitation of human left ventricular mass and volume by two-dimensional echocardiography: In vitro anatomic validation. *Circulation* 1981;63:1398-1407
38. Helak JW, Plappert T, Muhammad A, Reichek N: Two-dimensional echographic imaging of the left ventricle: Comparison of mechanical and phased-array systems in vitro. *Am J Cardiol* 1981;48:728-735
39. Linker DT, Pearlman AS, Lewellen TK, Huntsman LH, Moritz WE: Automated endocardial definition of two-dimensional echocardiograms: A comparison of four standard edge detectors and improved threshold techniques. *Comput Cardiol, IEEE* 1982: 395-398
40. Melton HE Jr, Skorton DJ: Rational gain compensation in cardiac ultrasonography. *Ultrason Imaging* 1983;5:214-228